H. Ugail

Partial Differential Equations for Modelling Wound Geometry

Book Series Studies in Mechanobiology, Tissue Engineering and Biomaterials

ISSN 1868-2006 (Print) 1868-2014 (Online)

Volume Volume 1

Book Bioengineering Research of Chronic Wounds

Publisher Springer Berlin Heidelberg

DOI 10.1007/978-3-642-00534-3

ISBN 978-3-642-00533-6 (Print) 978-3-642-00534-3 (Online)

Part II

DOI 10.1007/978-3-642-00534-3_5

Pages 101-125

Subject Collection Engineering

SpringerLink Date Wednesday, November 18, 2009

Partial Differential Equations for Modelling Wound Geometry

Hassan Ugail
School of Computing, Informatics and Media
University of Bradford, Bradford BD7 1DP
United Kingdom
h.ugail@bradford.ac.uk

Abstract

Wounds arising from various conditions are painful, embarrassing and often requires treatment plans which are costly. A crucial task, during the treatment of wounds is the measurement of the size, area and volume of the wounds. This enables to provide appropriate objective means of measuring changes in the size or shape of wounds, in order to evaluate the efficiency of the available therapies in an appropriate fashion. Conventional techniques for measuring physical properties of a wound require making some form of physical contact with it. We present a method to model a wide variety of geometries of wound shapes. The shape modelling is based on formulating mathematical boundary-value problems relating to solutions of Partial Differential Equations (PDEs). In order to model a given geometric shape of the wound a series of boundary functions which correspond to the main features of the wound are selected. These boundary functions are then utilised to solve an elliptic PDE whose solution results in the geometry of the wound shape. Thus, here we show how low order elliptic PDEs, such as the Biharmonic equation subject to suitable boundary conditions can be used to model complex wound geometry. We also utilise the solution of the chosen PDE to automatically compute various physical properties of the wound such as the surface area, volume and mass. To demonstrate the methodology a series of examples are discussed demonstrating the capability of the method to produce good representative shapes of wounds.

1. Introduction

Wounds, especially those related to chronic conditions such as pressure ulcers, venous ulcers, and diabetic ulcers are painful, embarrassing and

costly. A given wound may typically range in size from around 0.5 cm to 10 cm across and is of variable depth. The wound can be deeply undermined with the cavities ranging in size up to several cubic centimetres. Figure 1 shows two examples of wounds, one showing a deep foot ulcer relating to a chronic condition and the other showing several wounds on a human arm shape.

In the USA the estimated annual cost of pressure ulcer treatment alone range between $3.5 and $7 billion [1,2,3]. In the UK it is conservatively estimated that wounds relating to venous ulceration alone affects around 580,000 individuals at any one time of which a significantly high proportion are the elderly [4,5]. This prevalence imposes a significant burden on healthcare systems, with an approximate cost of between £300 and £600 million per year. A single Vascular Unit in England sees some 300-400 patients weekly, at an annual cost of £0.25million. The cost is not just financial: wounds take a toll in missed workdays and chronic unemployment because painful, open wounds disqualify people from many lines of work and many patients suffer damaging psychological side-effects. Many patients are treated at home by community nurses. For example, over 60% of treatment costs are for community nursing services [6]. Community nurses may spend 44% of their time dressing and providing care [7], yet treatment often remains ineffective [8,9] and considerable uncertainty remains regarding the most effective treatments [10].

Figure 1. Example wounds, a deep foot ulcer related to a chronic condition and deep wounds on an arm.

There exist a number of modalities to treat wounds. At any given setting these days, for wound care it requires rapid, highly reliable, low cost as

well as accurate methods of assessing wound dimensions. From a diagnostic point view in order to properly assess a given wound it requires an understanding of the 3-dimentional geometric shape of the wound. Without any accurate and objective means of measuring changes in size or shape of wound, it is difficult or impossible to properly evaluate the efficiency of the available therapies [11,12,13].

A crucial task, during the treatment of wounds, especially those that are considered chronic, is the measurement of their area and volume [11,13]. This enables to provide appropriate objective means of measuring changes in the size or shape of wounds, in order to evaluate the efficiency of the available therapies in an appropriate fashion. At the moment there appears to exist a number of measurement methods which are used clinically. Of which the most widely used methodology is the direct contacting measurements which are not accurate, carry a risk of infection and uncomfortable to the patient.

Conventional techniques for measuring the area and volume of wounds depend on making physical contact with the wound, for example by drawing around the periphery on an acetate sheet or by making an alginate cast of the wound [6]. For commonly used objective measures of wound healing the use of planimetric and two dimensional methods are very common. Methods of measuring wound dimensions often involve the direct measurements with the use of a ruler [14]. The ruler enables a quick and easy way to measure the wound whereby quantities such as the length, width and the depth of the wound is estimated [15]. Other common methods include the hand tracing of the perimeter of the wound with use of a grid to calculate wound area. Computer based wound documentation systems such as MAVIS (Measurement of Area and Volume Instrument System, Photometrix Imaging Ltd, Mid Glamorgan, UK), allow digital wound tracing [16]. Here the tracing of the wound boundary is undertaken by following the wound edge with a mouse cursor on a digital photograph of the wound.

There is currently significant interest in developing non-invasive measurement systems using optical methods such as ‘structured light’ (a technique that projects stripes on to a surface and infers the shape from changes in the linearity of the reflected stripe) or stereophotogrammetry [9,16,17]. The availability of high-resolution 3D digital cameras, increasing computing power and the development of software techniques for manipulating three-dimensional information has benefited this area. However, equipment associated with these sorts of measurement methods is

not often portable and is often costly, thus making the prohibitive for routine medical use. Nevertheless this is probably the most exhaustive mechanism for representation of the geometry of wound surface which is based on the reconstruction of the surface geometry in 3-dimensional space. This enables accurate calculation of the surface area and volume of the wound.

Here we address a possible approach that would enable to model and measure the geometry of complex wound geometry. The idea behind is based on shape parameterisation. In parametric design the basic approach is to develop a generic description of an object or a class of objects in which the shape is controlled by the values of a set of design variables or parameters. A new design, created for a particular application, is obtained from this generic template by selecting particular values for the design parameters so that the item has particular properties suited to that application. Thus, one could envisage a scenario where a generic parameterised 3-dimensional shape of a wound is available for a user where the user would be then able to create a fine tuned model based on a handful of direct measurements taken from a patient.

There exists a wide variety of methods that can be utilised to generate the geometry of wounds. Examples include boundary based methods such as polygon based design [18], extrusions and surface of revolution [19] and polynomial patches [20], procedural modelling such as implicit surfaces [21] and fractals [22] and volumetric models such as constructive solid geometry [23] and subdivision [24]. Many of these techniques, especially polygon based design and polynomial patches, would be appropriate for modelling the geometry of wounds.

Of the above mentioned techniques many commercial Computer Aided Design (CAD) systems today employ the conventional polynomial geometry modelling schemes. One of them is spline based schemes now dominated by Non Uniform Rational B-Splines (NURBS) [25,26]. There has been a considerable amount work undertaken in the area of geometry representation using NURBS. An example of geometry representation using spline based methods has been developed by Piegl [27, 28]. The example describes how the geometry of a brush handle can be designed by using a series of cross sectional profile curves. For this problem, the points per cross section were taken between 10 to 48 and the number of control points after merging all the surface patches were nearly 4000. In addition to the 4000 control points, one also has to take into account the associated weights of the spline functions that are used. In a similar fashion Pottmann

[29] describes the approximation of a ruled cylindrical surface using NURBS. Here a surface of bi-degree with 7×25 control points were utilsed.

Thus, conventional geometry modelling techniques based on splines are not suitable to overcome geometry parameterisation problems since such methods typically use polynomial patches (e.g. Non Uniform Rational B-Splines or NURBS), which often require hundreds of control points in order to represent a realistic object. Furthermore, such "spline" based patches often do not exactly meet at the boundaries and consequently need to be 'trimmed' or stitched in order to close the geometry of the object in question.

Triangular meshes or subdivision schemes [30,31,32] for geometry representation has recently been popular as an alternative to spline based techniques. For example, Hubeli and Gross [33] describe a geometric surface in which Doo-Sabin subdivision scheme is applied on a two manifold surface to represent its geometry. In order to reconstruct the geometry of the shape they have utilized around 50 smoothing steps using the subdivision method. Similarly, Catmull [34] reconstruct a teapot using his subdivision algorithm. Although being much more flexible than spline based techniques, triangular meshes also have restrictions and disadvantages. For example, when applying an extreme deformation to a triangle mesh, certain triangles exhibit strong stretching which leads numerically and visually undesirable triangles that have to be overcome.

Geometry based on Partial Differential Equations (PDEs) have recently emerged as a powerful tool for geometric shape modelling [35,36,37,38,39]. Using this methodology, a surface is generated as the solution to an elliptic Partial Differential Equation (PDE) using a set of boundary conditions. The PDE method is efficient in the sense that it can represent complex three-dimensional geometries in terms of a relatively small set of design variables.

Mathematical boundary-value problems such as the use of elliptic Partial Differential Equations (PDEs) are well known for their application in many engineering problems including stress/stain analysis, fluid flows and electromagnetism. From a geometric design point of view such boundary-value problems have found their way into various application areas such as surface design, geometric mesh smoothing and fairing. To this end it is noteworthy to refer to Bloor and Wilson’s PDE method [40, 37, 41], for intuitive shape generation. This method is based on the solution of the Bi-

harmonic PDE with appropriately chosen boundary conditions. We also take note of the work by Schneider and Kobbelt and others on geometric mesh fairing [42, 43, 44], where the properties of the Biharmonic operator is used to fair triangular meshes. Other PDE based techniques in geometric design include level set formulations for image processing, computer graphics and computer vision [45,46,47] geometric mesh processing [48, 49] and Radial Basis Functions [50]. Such PDE based techniques form well posed problems as well as possess appealing functionality in terms of their solution being smooth functions whereby such solutions can be controlled by the specified boundary conditions.

The advantage of the geometry based on PDEs is that it can represent complex geometry in terms of a small set of design variables [51], instead of many hundreds of variable using traditional modelling techniques. In broad terms this is because its boundary-value approach means that PDE geometry are defined by data distributed around just their boundaries, instead of data distributed over their surface area, e.g. control points. The method defines a shape in terms of a number of surface patches that collectively describe the object's surface. However, unlike spline-based approaches, the method produces surface patches that exactly meet at their mutual boundaries, without the need for complicated trimming. Thus, a PDE model, when changed by altering the values of its design parameters, remains continuous; there is no need for a designer to intervene in order to close up any holes that might appear at patch boundaries. In the present context, this means that the PDE geometry can be made to adapt automatically to changes in the shape of the wound in question.

2. Elliptic Partial Differential Equations for Shape Modelling

In very simple terms, one can describe Partial Deferential Equations (PDEs) as a mathematical tool that can be used to describe a given physical phenomena. This description is given in the form of a mathematical relation between different rates of change of the phenomena in study with respect to different variables such as the 3-dimentional physical coordinates or time. The range of application areas that form the use of PDEs vary from physical phenomena such as fluid flow applications such as weather forecasting to economics and finance.

The subject of PDEs holds an exciting and special position in applications relating to modelling physical phenomena. PDEs emerged as a subject in the 18th century due to the failure of ordinary differential equations to describe physical phenomena. The subject of PDEs has been developed by major names in applied mathematics such as Euler, Legendre, Laplace and Fourier. For example, Euler and Laplace developed the idea of potential theory [52] while Fourier developed series expansions for heat equation. Many advances in modern science have been based on the discovery of the underlying PDE for the process in question. Examples include Maxwell's equations [53] which describe a unified theory between electricity and magnetism, the Schrödinger's equation for quantum mechanics and Navier-Stokes' equation [54] for modelling fluid flows with applications to weather forecasting, motion of stars inside galaxies and flow around aerofoil wings.

Mathematically speaking, these rates of change are known as derivatives and in particular, these rates are known as partial derivatives when the function that is being differentiated depends on two or more variables. For instance, assume that a function F depends on x, y and t; that is, $F(x, y, t)$ where $0 \le x \le 1,\ 0 \le y \le 1$ and $t \ge 0$. The rate of change of F with respect to x denoted as $\frac{\partial F}{\partial x}$ which represents the partial derivative of F with respect to x. Now if we are to represent the rate of change of $\frac{\partial F}{\partial x}$ with respect to y we can denote this as $\frac{\partial^2 F}{\partial x \partial y}$.

Assuming that a given physical phenomenon can be mathematically modelled using F where the phenomenon is governed by the relation between its rate of change with respect to the variables x and y and a function $G(x, y, t)$, we can write such a PDE as,

$$\frac{\partial F}{\partial x} + \frac{\partial^2 F}{\partial x \partial y} = G(x, y, t). \tag{1}$$

2.1 Classification of Partial Differential Equations

It is common practice in mathematics to use a quantity called the discriminant for determining the nature of the roots associated with a given second order algebraic equation. The discriminant could tell if both the roots are real and different, if there is only one root or if they are complex. Simi-

larly, PDEs can be classified into different types of equations depending on the value of the discriminant. If one assumes that the general second order partial deferential equation in two variables is given by,

$$A\frac{\partial^2 F}{\partial^2 x}+B\frac{\partial^2 F}{\partial x\partial y}+C\frac{\partial^2 F}{\partial^2 y}+...,\tag{2}$$

then the discriminant of the Equation (2) can be written as,

$$B^2-4AC.\tag{3}$$

The classification is divided into three major groups. i.e.,

1. $B^2-4AC<0$

PDEs fulfilling this condition are regarded as elliptic partial differential equations. An example of elliptic partial differential equations is the Laplace equation. The solutions of these types of PDEs are generally given in terms of harmonic functions and are smooth within the domain in which they are solved. Moreover, if the coefficients multiplying the terms involving the unknown function and its derivatives are separable, the solution can be found using Fourier transforms. The aim of this work is to enhance the use of elliptic PDEs as a surface and solid generation technique relating to wound geometry. Thus, further details of specifically selected low order elliptic PDEs would be the main theme of discussion of this paper.

2. $B^2-4AC>0$

Any second order PDE satisfying this condition is classified as a parabolic PDE. The heat equation is an example of a parabolic equation. Parabolic PDEs are typically related to evolution problems such as heat diffusion. For that reason they are also known as evolution equations since they describe how a physical property changes through time across a given domain. Generally, the solution to this type of an equation is less stable than those to elliptic PDE i.e. they reach a singularity as they evolve with time.

3. $B^2-4AC=0$

Any PDE satisfying the above condition is called a hyperbolic PDE. An example of such a type PDE is the wave equation.

2.2 The Biharmonic Equation

In this work we are placing special emphasis on the Biharmonic PDE which is utilised to be the basic building block for modelling the wound geometry. The Biharmonic PDE falls into the category of elliptic PDEs of the type commonly denoted by,

$$(\nabla^2)^k F = 0, \tag{4}$$

where ∇^2 represents the Laplace operator and $k \geq 1$. The form of Laplace operator in a Cartesian 3-dimentional coordinate system is denoted as,

$$\nabla^2 = \frac{\partial^2 F}{\partial^2 x} + \frac{\partial^2 F}{\partial^2 y} + + \frac{\partial^2 F}{\partial^2 z}. \tag{5}$$

The case when $k = 2$ Equation (4) is known as the Biharmonic equation. Its solution is given in terms of functions whose fourth partial derivatives are continuous and satisfy the Biharmonic condition. Examples in which this equation has played an important role describing physical phenomena are the case of stokes flows in fluid dynamics, where the Biharmonic equation is used and the stream function describing the flow or in continuum mechanics where it is used to find the Airy or Love stress functions to describe plane stress or pane strain problems in order to find the displacement function.

In order to solve the Biharmonic PDE, or for that matter any PDE, a number of boundary conditions are usually required. The nature of the boundary conditions required to solve the equation depends on the type of problem and in general there are two types of boundary conditions. They are Dirichlet boundary conditions and he Neumann boundary conditions. The Dirichlet boundary conditions specify the value of F on the boundary of the region in which the solution wants to be found. The Neumann boundary conditions specify the value of the normal derivative of the function F at the boundary of the domain.

2.3 The Solution of the Biharmonic Equation

The solution to the Biharmonic equation can be found through a number of techniques. Full analytic solution can be found in some cases but it also has been solved using numerical techniques, which in general tend to provide very stable results. This is attributed to the fact that the discrete formulation of the Laplace equation is regarded as an averaging process.

The task of finding a solution to the Biharmonic equation is by no means trivial. Sometimes with a suitable choice of boundary conditions and restriction placed on the domain of the solution one can obtain a simple analytic solution to the equation. However, in the vast majority of cases this is not the case and often approximate solutions based on numerical analysis are sought. Here we outline the common methods that can be employed to find solution of the Biharmonic equation subject to a given set of boundary conditions.

2.3.1 Analytic Methods

Among the popular analytic methods available for finding the solution of the Biharmonic equation involves the use of separation of variables. This method is generally used to solve linear PDEs and consists of expressing the unknown function in terms of a product of a series of functions, each of which depend only and only on one of the independent variables.

2.3.2 Spectral Methods

These methods usually express the solution of the PDE in terms of its Fourier series, which is then substituted in the PDE itself in order to obtain a system of ordinary differential equations. This simplifies the problem. However it is often necessary to employ numerical techniques to find the solution to each ordinary differential equation.

2.3.3 Numerical Methods

The most common of numerical methods employed in solving Biharmonic PDE is the finite differences, finite element method and element of boundary. Below, a brief description of each of these techniques is given.

- Finite difference method

Finite difference methods are based on grid-type discretisation of the unknown function in the domain in which the solution to the PDE is to be found. The derivatives involved in the Biharmonic equation are then ex-

pressed in terms of these discrete points according to well established rules at every point in the grid and as many neighbouring points as required by the order of the derivative in turn. It is worth mentioning that the value of the function and its derivatives are also expressed in the same manner but are somehow compensated with the boundary conditions. Then, all the corresponding expressions are substituted in the original PDE, leading to a system of algebraic equations that can be easily solved. Finite difference methods can be further categorised into explicit, implicit and semi-implicit methods. The type of method selected to solve a particular PDE depends on criteria often related to the inner stability of the method.

- Finite element method

The working principle of this technique consists of approximating the original Biharmonic equation into a system of ordinary differential equations that can be integrated numerically using well known methods. The main challenge when applying this technique to consist of approximating the original equation in order to ensure the solution is stable.

- Boundary element method

This method consists of finding a suitable set of boundary values from the integral equation resulting from formulating the original Biharmonic equation in integral form. The boundary values found can then be used to calculate the numerical solution of the original PDE. Finite element methods are regarded as accurate; however, they usually lead to very large matrix systems and therefore their computational cost is quite high.

3. Modelling wound geometry

In this paper we utilise the elliptic PDE known as the Biharmonic equation in order to model the geometry of wound shapes. The aim here is to show how a boundary-value approach can be adopted to model complex geometry corresponding to wound shapes intuitively. The Biharmonic equation when solved subject to suitable boundary conditions enables to define complex geometry in terms of a small set of design variables [51]. This is because the boundary-value adopted here surfaces are defined by data distributed around just their boundaries, instead of data distributed over their geometry.

In the current context the PDE geometry we want to model can be regarded as a parametric surface patch $\underline{X}(u,v)$, defined as a function of two parameters u and v on a finite domain $\Omega \subset R^2$, by specifying boundary data around the edge region of $\partial\Omega$. Typically the boundary data are specified in the form of $\underline{X}(u,v)$ and a number of its derivatives on $\partial\Omega$. Here one should note that the coordinate of a point u and v is mapped from that point in Ω to a point in the physical space. To satisfy these requirements the surface $\underline{X}(u,v)$ is regarded as a solution of a PDE of the form,

$$\left(\frac{\partial^2}{\partial u^2}+\frac{\partial^2}{\partial v^2}\right)^2 \underline{X}(u,v)=0, \tag{6}$$

The PDE given in Equation (6) is of fourth order. Therefore, in order to solve the Equation, four boundary conditions are required. Here four positional curves are taken as the four boundary conditions.

Let Ω be a finite domain defined as $\{\Omega : 0 \le u \le 1, 0 \le v \le 2\pi\}$ such that,

$$\begin{aligned}
\underline{X}(0,v) &= \underline{P}_0(v),\\
\underline{X}(s,v) &= \underline{P}_s(v),\\
\underline{X}(t,v) &= \underline{P}_t(v),\\
\underline{X}(1,v) &= \underline{P}_1(v),
\end{aligned} \tag{7}$$

where $\underline{P}_0(v)$ and $\underline{P}_1(v)$define the edges of the surface at $u=0$ and $u=1$ respectively. $\underline{P}_s(v)$ and $\underline{P}_t(v)$ are the positions of the second and third functions as described in Equation (7). Here s and t are the positions of the interior curves such that, $0 \le s < t,$ and $s < t \le 1$.

Using the method of separation of the variables, the explicit solution of Equation (6) can be written as,

$$\underline{X}(u,v)=\underline{A}_0(u)+\sum_{n=1}^{\infty}\{\underline{A}_n(u)\cos(nv)+\underline{B}_n(u)\sin(nv)\}, \tag{8}$$

where,

$$\underline{A}_0 = \underline{a}_{00}+\underline{a}_{01}u+\underline{a}_{02}u^2+\underline{a}_{03}u^3, \tag{9}$$

$$\underline{A}_n(u) = \underline{a}_{n1}e^{nu} + \underline{a}_{n2}ue^{nu} + \underline{a}_{n3}e^{-nu} + \underline{a}_{n4}ue^{-nu}, \quad (10)$$

$$\underline{B}_n(u) = \underline{b}_{n1}e^{nu} + \underline{b}_{n2}ue^{nu} + \underline{b}_{n3}e^{-nu} + \underline{b}_{n4}ue^{-nu}, \quad (11)$$

where $\underline{a}_{00}, \underline{a}_{01}, \underline{a}_{02}, \underline{a}_{03}, \underline{a}_{n1}, \underline{a}_{n2}, \underline{a}_{n3}, \underline{a}_{n4}, \underline{b}_{n1}, \underline{b}_{n2}, \underline{b}_{n3}$ and $\underline{b}_{n4}$ are vector valued constants, whose values are determined by the imposed boundary conditions at $u = 0, u = s, u = t$ and $u = 1$.

For a given set of boundary conditions, in order to define the various constants in the solution, it is necessary to perform Fourier analysis of the boundary conditions and identify the various Fourier coefficients. For a finite number of Fourier modes N (e.g. $4 \le N \le 10$) the approximate surface solution can be defined as,

$$\underline{X}(u,v) = \underline{A}_0(u) + \sum_{n=1}^{N} \{\underline{A}_n(u)\cos(nv) + \underline{B}_n(u)\sin(nv)\} + \underline{R}(u,v), \quad (12)$$

where $\underline{R}(u,v)$ is called a remainder function defined as,

$$\underline{R}(u,v) = \underline{r}_1(v)e^{wu} + \underline{r}_2(v)ue^{wu} + \underline{r}_3(v)e^{-wu} + \underline{r}_4(v)ue^{-wu}, \quad (13)$$

where $\underline{r}_1, \underline{r}_2, \underline{r}_3, \underline{r}_4$ are obtained by considering the difference between the original boundary conditions and the boundary conditions satisfied by the function,

$$\underline{F}(u,v) = \underline{A}_0(u) + \sum_{n=1}^{N} \{\underline{A}_n(u)\cos(nv) + \underline{B}_n(u)\sin(nv)\}, \quad (14)$$

and $w = \dfrac{1}{N+1}$.

The remainder function $\underline{R}(u,v)$ is calculated by means of the difference between the original boundary conditions and the boundary conditions satisfied by the function $\underline{F}(u,v)$ therefore it guarantees that the chosen boundary conditions are exactly satisfied [55]. Note that the terms $\underline{r}_j$ are vector valued functions depending on the parametric coordinate v. Another thing to point out is that it is necessary to express the boundary conditions defining the particular solution to Equation (12) in terms of the corresponding Fourier series.

Once the boundary conditions are expressed in terms of a Fourier series, the values of a_{ij} and b_{ij} can be found. For this purpose, a series of systems of linear equations need to be solved. These systems are of the form,

$$Mx = c, \tag{15}$$

where M represents the matrix associated with the system, x denotes the unknown of such a system and c is the independent value of each algebraic equation in the system. In particular, the system to be solved to find the solution to Equation (12) is given by,

$$\begin{aligned} M_0 x_{A0} &= c_{A0}, \\ M_{0n} x_{An} &= c_{An}, \\ N_n x_{Bn} &= c_{Bn}, \end{aligned} \tag{16}$$

where M_0, M_n and N_n are matrices. The subscripts in these matrices denote the system with which they are associated with. For instance, M_0 is the matrix associated with the term A_0 in Equation (9), whilst M_n and N_n are linked to the terms A_n and B_n respectively. The vectors x_{A0}, x_{An} and x_{Bn} represent the unknowns in the system associated with each respective term in Equation (10) and (11). Finally, the independent vectors c_{A0}, c_{An} and c_{Bn} determined by the boundary conditions.

The matrices are thus given by,

$$M_0 = \begin{pmatrix} 1 & 0 & 0 & 0 \\ 0 & 1 & 0 & 0 \\ 1 & 1 & 1 & 1 \\ 0 & 1 & 2 & 3 \end{pmatrix}, \tag{17}$$

$$M_n = N_n \begin{pmatrix} 1 & 0 & 1 & 0 \\ n & (1+n) & -n & (1-n) \\ e^n & e^n & e^{-n} & e^{-n} \\ ne^n & (1+n)e^n & -ne^{-n} & (1-n)e^{-n} \end{pmatrix}. \tag{18}$$

The vectors x_{A0}, x_{An} and x_{Bn} and are defined by,

$$x_{A0} = (a_{00}, a_{01}, a_{02}, a_{03}),$$

$$x_{An} = (a_{n1}, a_{n2}, a_{n3}, a_{n4}), \tag{19}$$

$$x_{Bn} = (b_{n1}, b_{n2}, b_{n3}, b_{n4}).$$

As mentioned before, the independent vectors c_{A0}, c_{An} and c_{Bn} are determined by the boundary conditions; that is, they are associated with the Fourier series of all the boundary conditions. Let ca_{i1}, $ca_{i2}, ca_{i3}, ca_{i4}$ cb_{i1}, cb_{i2}, cb_{i3} and cb_{i4} represent the coefficients associated with the Fourier series of each of the boundary conditions respectively. Thus, the independent vectors are defined by,

$$c_{A0} = (ca_{00}, ca_{01}, ca_{02}, ca_{03}),$$

$$c_{An} = (ca_{n1}, ca_{n2}, ca_{n3}, ca_{n4}), \tag{20}$$

$$c_{Bn} = (cb_{n1}, cb_{n2}, cb_{n3}, cb_{n4}).$$

The next and final step to find the solution to Equation (12) is therefore to solve the systems of equations previously defined. This can be done using readily available algorithms [56]. Note that the number of systems to be solved in this fashion is equal to $2N+1$. Although the constants required to determine $R(u,v)$ are calculated in a similar manner, the number of systems to be solved depend on the resolution assigned to the v direction. for instance, if the solution of Equation (12) is to be calculated over a uv mesh of 20 by 20 points, then 20 systems would be solved to obtain the full solution. This is due to the dependency of the remainder term on v.

3.1 Examples of PDE geometry

In this section we discuss some of examples which show how the geometry based on solutions of PDEs can be generated. We choose the Biharmonic equation given in (6) and the boundary conditions are taken in the format described in Equation (7).

As a first example we show how a fourth order PDE surface is generated where all the conditions are taken to be function conditions. Fig. 2(a) shows the boundary conditions to solve the Biharmonic PDE. Fig. 2(b) shows the shape of a surface generated by the fourth order PDE where the conditions are specified in terms of the curves shown in Fig. 2(a). In particular, the conditions are such that, $X(0,v) = c_1(v)$, $X(1/3,v) = c_2(v)$, $X(2/3,v) = c_3(v)$ and $X(1,v) = c_4(v)$. Since we are taking four function conditions to solve the fourth order PDE, all the curves in this case lie on the resulting surface. Thus, in this particular case the resulting PDE surface is a smooth interpolation between the given set of functional conditions.

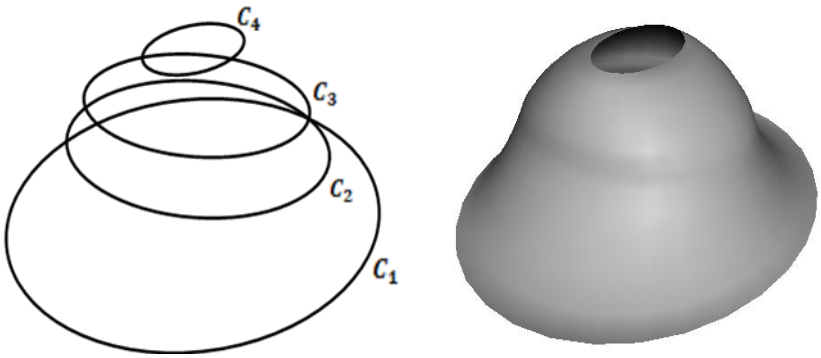

(a) **(b)**

Figure 2. The shape of a surface generated by the fourth order PDE where the conditions are all taken to be function conditions. (a) The conditions defined in the form of curves in 3-space. (b) The resulting surface shape.

As a second example we show how a four sided patch can be generation as the solution to the Biharmonic equation. Again here all the conditions are taken to be function conditions. Here Fig. 3(a) shows the necessary boundary conditions to solve PDE. Fig. 3(b) shows the shape of a surface generated by the fourth order PDE where the conditions are specified in terms of the curves shown in Fig. 3(a). In particular, the conditions are such that, $X(0,v) = c_1(v)$, $X(1/3,v) = c_2(v)$, $X(2/3,v) = c_3(v)$, $X(1,v) = c_4(v)$. Note here the parameter range for u and v such that, $0 \le u \le 1$ and $0 \le v \le \pi$. Since we are taking four function conditions to solve the fourth order PDE, all the curves in this case lie on the resulting

surface. Thus, in this particular case the resulting PDE surface is a smooth interpolation between the given set of functional conditions.

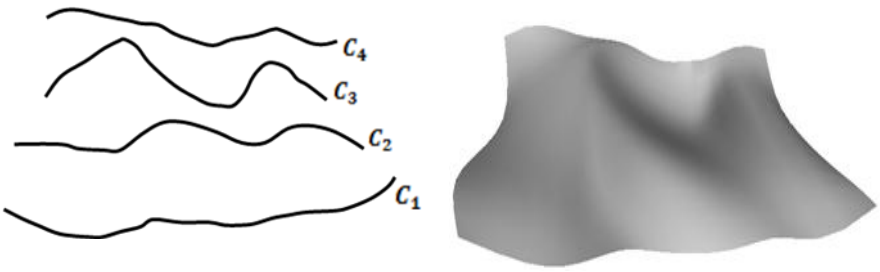

Figure 3. A four-sided surface patch generated by the fourth order PDE where the conditions are all taken to be function conditions. (a) The conditions defined in the form of curves in 3-space. (b) The resulting surface shape.

The above two examples how solutions of PDEs based on the 4th order Biharmonic equation enables to generate surface shapes. As discussed above, the basic idea here is to generate a series of curves that can be utilised to define the boundary conditions for the chosen PDE. As seen in the examples, the resulting surface shape can always be intuitively predicted from the shapes of the chosen curves.

3.2 Modelling geometry of wound shapes

Here we show how the above describe technique can be utilised to generate a wide range of shapes which correspond to wound geometries. The idea here is to show how generic shapes of wounds (both the surface of the wound and the interior part of the wound) can be generated based on the above techniques. In what follows we first discuss how the surface of a wound can be modelled using the Biharmonic equation. We then adopt the technique for generating enclosed surface which correspond to the interior shape of the wound.

3.2.1 Modelling surface geometry of wounds

In this subsection we describe how the surface of a would can be created using the solution to the Biharmonic equation as described earlier. As usual, we generate four boundary curves through which we seek an interpolation (corresponding to the surface of the wound) based on the Bihar-

monic equation. The curves are defined as splines of the form $P_i = \sum_i C_i B_i$ where B_i is a cubic polynomial and C_i are the corresponding control points. Thus, the curves once defined through spline form are discretely sampled in order to obtain their Fourier representations so that the analytic solution outlined previously can be utilised.

Fig. 4(a) shows typical boundary conditions for the chosen PDE. Fig. 4(b) shows an example wound surface where Fig. 4(a) shows the corresponding curves utilised to generate the surface shapes. Here the boundary conditions are defined as periodic functions such that $X(0,v) = c_1(v)$, $X(0.3,v) = c_2(v)$, $X(0.7,v) = c_3(v)$ and $X(1,v) = c_4(v)$. Note that the curve $c_4(v)$ in this case is a point in 3-space whose Fourier representation is utilised as one of the boundary conditions for the PDE.

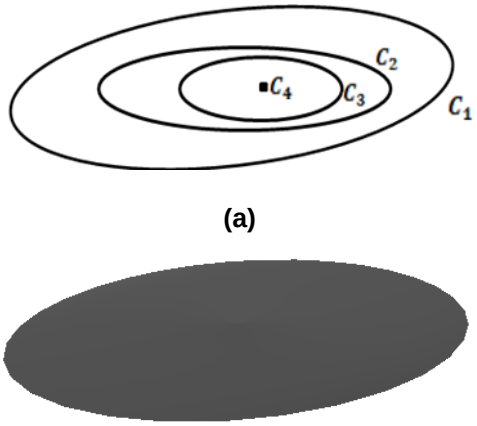

(a)

(b)

Figure 4. An example wound surface generated by the fourth order PDE where the conditions are all taken to be function conditions. (a) The conditions defined in the form of curves in 3-space. (b) The resulting wound surface shape.

Fig. 5 shows further examples of wound surface geometry generated using the above described methodology. In each case the boundary conditions are similar to that shown in Fig. 4(a) where each of the boundary conditions is defined as a spline function. The corresponding control points of the spline are manipulated in real-time in order to generate alternative

shapes of boundary curves resulting alternative shapes of wound surface geometry.

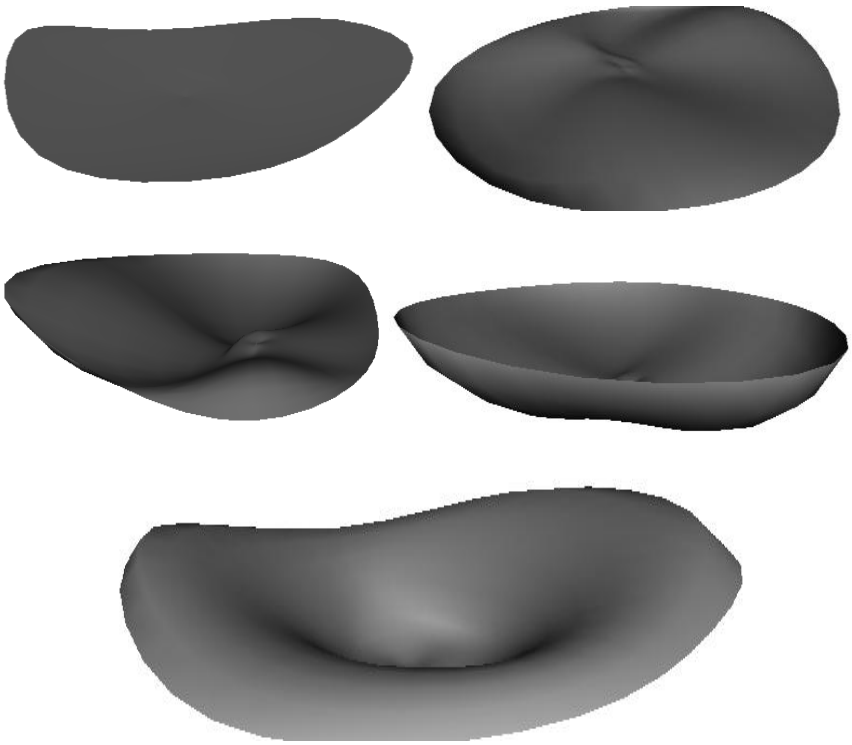

Figure 5. Example wound surface geometry generated by using the Biharmonic equation. In each case the surface geometry is generated by manipulating the boundary conditions through the control points of the spline functions.

3.2.2 Modelling the interior geometry of wounds

In this section we show how the PDE based methodology can be utilised to generate the interior geometry of the wound shapes. Like the surface of the wounds, the interior shapes are equally important and therefore being able to model the interior part of a wound is paramount. Fig. 6(a) shows the boundary conditions required to solve the PDE. Fig. 6(b) shows a generic shape of wound which has been created using two fourth order Biharmonic surface patches with a common boundary. Fig. 6(a) shows the boundary curves corresponding to this shape. Here we generate two surface patches,

one for the curves $c_1(v)$, $c_2(v)$, $c_3(v)$ and $c_4(v)$ and the other for the curves $c_4(v)$, $c_5(v)$, $c_6(v)$ and $c_7(v)$. Thus, $c_4(v)$ is taken to be a common boundary where both the surface patches meet. Again the curves $c_1(v)$ and $c_7(v)$ are taken to be point in 3-space. Note also that all the curves are defined as spline functions whose control points can be utilised to manipulate the curves in 3-space.

With the above formulation, the analytic solution is utilised to generate the geometry shown in Fig. 6(b).

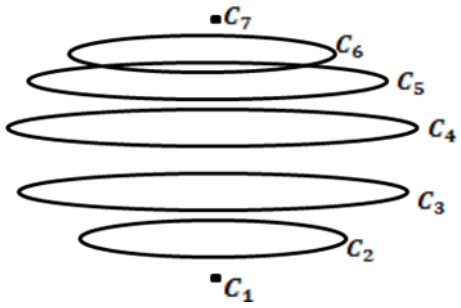

(a)

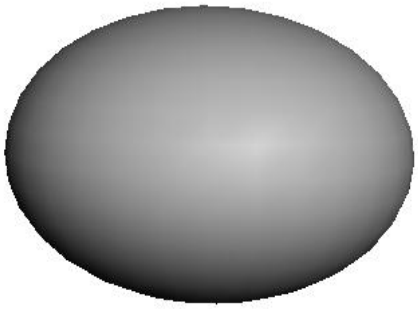

(b)

Figure 6. An example geometry corresponding to the interior of a wound generated as a two blended fourth order PDE surface patches. (a) The boundary conditions defined in the form of curves in 3-space. (b) The resulting wound geometry shape.

Figure 7 shows further examples of wound geometry generated using the above described methodology. In each case the boundary conditions are similar to that shown in Fig. 6(a) where each of the boundary conditions are defined as spline functions. The corresponding control points of the spline are manipulated in real-time in order to generate alternative shapes of boundary curves, resulting in the shapes of wound geometry as shown.

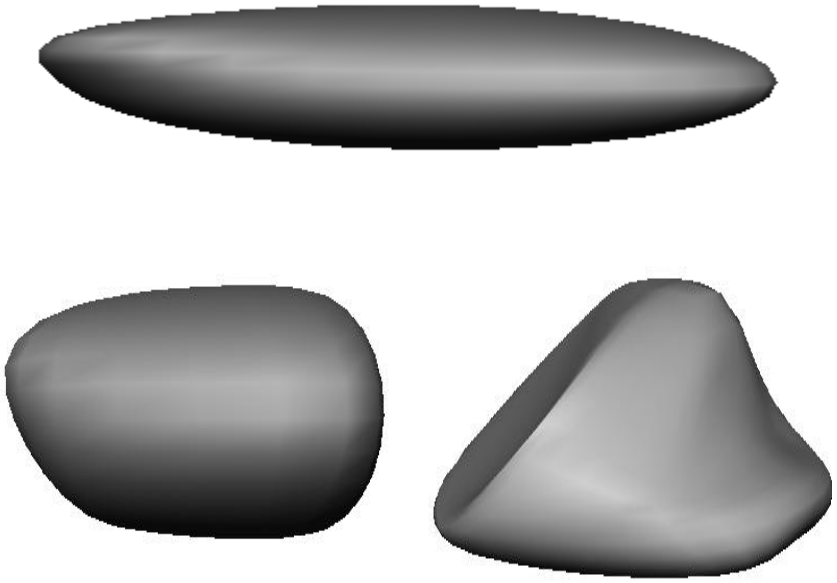

Figure 7. Example geometries corresponding to the interior of typical wounds. In all cases the geometry is generated by means of manipulating the boundary conditions defined Fig (a), in real-time.

4. Measuring properties of wounds

In this section we discuss how PDE based geometry modelling techniques can be coupled with computational techniques in order to measure various properties of wounds. Properties such as the surface area, enclosed volume and mass of the wound may be of use by clinicians in order to characterise the wound and estimate the healing properties of various therapies. We

show how the geometry generated by PDE surfaces can be directly utilised to compute physical properties of the wounds.

From the previous sections it is clear that we can generate a complex geometric shape of a wound as an analytic solution of a fourth order Biharmonic PDE. This means that we can define the geometry of a complex wound shape as a mathematical function. This function can thus be utilised to compute the physical properties of the wound.

4.1. Surface Area and Volume of the Wound Shape

As described in detail above, a surface $\underline{X}(u,v)$ defined over a finite domain Ω is utilised to describe the shape of the wound where $\underline{X}(u,v)$ is an analytic function defined as a solution of the Biharmonic equation subject to a suitable set of boundary conditions.

Then the surface area of the wound shape is given by,

$$A_w = \iint du dv\,, \tag{21}$$

and the volume enclosed by the wound is given by,

$$V_w = \iint dV, \tag{22}$$

where

$$dV = \underline{X}_u \wedge \underline{X}_v du dv. \tag{23}$$

Note here the subscript at $\underline{X}_u$ and $\underline{X}_v$ denote the partial differentiations.

The product in Equation (23) can be easily computed by means of the inverse of the Jacobian of the transformation J_v defined by,

$$J_v^{-1} = \begin{vmatrix} x_u & x_v \\ y_u & y_v \\ z_u & z_v \end{vmatrix}. \tag{24}$$

Hence, provided we are able to represent the wound shape closely by means of the choosing appropriate boundary data the surface area and volume of the wound can be automatically computed using the above technique. This eliminates invasive mechanisms for measuring properties of the wound such as the use of square based grids for estimating the surface area of the wound.

4.2. Mass Properties of the Wound

In some cases it may also be necessary to compute the mass properties of the actual wound. Here we propose a mechanism for computing the mass of the wound.

Assuming the wound under consideration is solid of uniform density we can model the solid geometry of the wound shape by means of the PDE,

$$\left(\frac{\partial^2}{\partial u^2} + \frac{\partial^2}{\partial v^2} + \frac{\partial^2}{\partial w^2} \right)^2 \underline{X}(u, v, w) = 0. \tag{25}$$

Equation (25) can be seen as a mapping from a solid cube parameterised by u, v and w to a solid. Subject to suitable boundary conditions, which can be determined from the surface of the wound geometry, Equation (25) can be solved to create the solid geometry of the wound. However, unlike the previous case of the Biharmonic equation defined over the parameter space u and v Equation (25) does not possess an analytic solution. Hence the equation now has to be solved numerically.

Given the surface geometry of a wound shape, suitable boundary conditions can be chosen for Equation (25) in order to generate the solid geometry corresponding to the wound. Given the function $\underline{X}$ defining the solid geometry of the wound one can compute the mass of the wound by the volume integral,

$$M_w = \iiint dxdydz. \tag{26}$$

As before, rather than calculating this quantity over the physical space we can transform it to the parametric domain where an element of volume is given by,

$$dV = (\underline{X}_u \wedge \underline{X}_v).\underline{X}_w dudvdw, \tag{27}$$

where, as before, the subscripts denote the partial differentiations. The triple product in Equation (27) is the inverse of the Jacobian of the transformation J_v defined by,

$$J_v^{-1} = \begin{vmatrix} x_u & x_v & x_w \\ y_u & y_v & y_w \\ z_u & z_v & z_w \end{vmatrix}. \tag{28}$$

Thus, the mass of the wound can be measured by means of evaluation the integral,

$$M_w = \iiint J_v^{-1} du dv dw. \tag{29}$$

It is noteworthy that in most cases the integral in Equation (29) has to be compute numerically with J_v being evaluated at suitable points over a unit cube.

5. An Example of Wound Modelling

In this section we show how a given wound geometry can be modelled using the methodology discussed above. Here we use 4th order PDE surface patches in order to model a wound shape by means of utilising real data.

Fig 8(a) shows the 3-dimentional geometry corresponding to the deep foot chronic ulcer shown in Figure 1. The surface data of the geometry was acquired using multiple-camera photogrammetry by means of the DSP400 system from 3dMD Ltd. This commercial technology has been widely used for acquiring medical images, especially in the USA, and captures data in a few milliseconds. The surface resolution (i.e. the separation of data points) is approximately 2mm with a positional accuracy of approximately 0.2mm.

In this example we show how we can generate the geometry corresponding to the foot and the corresponding wound shown in Figure 1. In order to generate a representative PDE surface shape, we extract a series of curves along the profile of the geometry model. For this purpose we import the scanned geometry mesh model into an interactive graphical environment through which we can examine and interact with the model. We then manually identify a number of regions on the scanned geometry model.

These regions are then utilised to determine the number of PDE surface patches required to produce a good representative model.

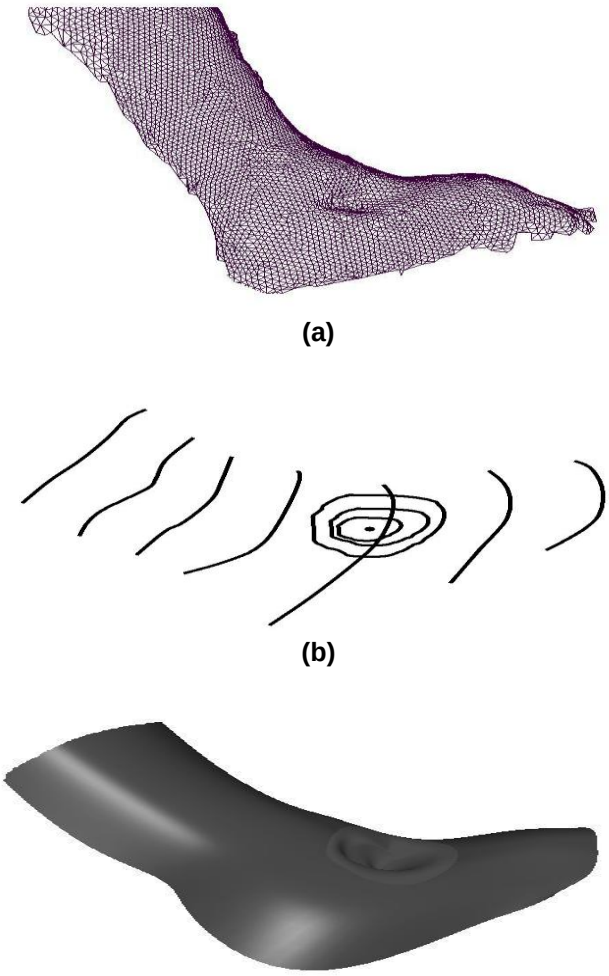

(a)

(b)

(c)

Figure 8. Example wound geometry modelling using PDEs.

The criteria in determining the number of PDE surface patches required is purely based on the required degree of accuracy by which one wants to approximate the scanned geometry using PDE surface patches. i.e. the

more the number of surface patches the higher the degree of accuracy. Once the number of surface patches required is decided then appropriate number of curves for each surface patch is extracted from the scanned geometry data. To do this we create a series of free-form cubic spline curves within the interactive environment. The spline curves are then projected onto the scanned geometry at the positions where the PDE boundary curves are to be extracted.

Fig. 8(b) shows the curves that have been extracted. First the curves corresponding to main foot is utilised to generate a smooth surface for the geometry of the foot (without the wound shape). In this case the foot surface is generated using two 4^{th} order PDEs with a common boundary. A portion of the geometry corresponding to the wound shape is then trimmed out from the main foot surface in order to accommodate the wound shape. The trimming process which we utilised for this purpose is outlined in [37]. Finally an additional 4^{th} order patch is generated for the wound shape as shown in Fig. 8(c).

The above example demonstrates how one can develop a practical system for measuring both the 3-dimentional shape and its associated properties which can be useful by clinicians and other medical staff working in the related areas. Such a system should have templates of generic PDE based wound shapes whereby the user can input a handful of key measurements taken from the wound. These key measurements should enable the system to generate appropriate boundary conditions to generate a close approximation of the wound shape and provide the relevant physical properties to the user.

6. Conclusions and Future work

Modelling wound geometry is a crucial task in order to evaluate the efficiency of the available therapies in an appropriate fashion. A crucial task, during the treatment of wounds, is the measurement of the size area and volume of the wounds.

Here we have presented a method to model a wide variety of geometries of wound shapes. The shape modelling is based on formulating mathematical boundary-value problems relating to solutions of Partial Differential Equations (PDEs). In order to model a given geometric shape of the wound a series of boundary functions which correspond to the main features of the wound are selected. These boundary functions are then utilised to solve an

elliptic PDE whose solution results in the geometry of the wound shape. Thus, here we show how low order elliptic PDEs, such as the Biharmonic equation subject to suitable boundary conditions can be used to model complex wound geometry. We also utilise the solution to automatically compute various physical properties of the wound such as the surface area, volume and mass. To show the practical ability of the methodology a series of examples are discussed demonstrating the capability of the method to produce good representative shapes of wounds.

In this work we have mainly utilised low order elliptic PDEs where the chosen PDE is solved subject to suitable boundary conditions. The work has potential for developing software tools whereby efficient geometry parameterisation of wounds can be undertaken by means of taking a small set of key measurements from given wounds. A description of a particular wound can be obtained from this generic template by assigning values for the parameters so that the model is matched to the given wound geometry. The assigned values – and hence the 'tailor-made model' – would be calculated from a small number of simple measurements taken from the patient, somewhat similar to the way in which a tailor or dressmaker obtains key measurements that determine the fit of bespoke clothing.

Another potential area to investigate would be the study of time-dependent PDEs where the geometric shape of the wound can be associated with its healing kinetics in order to model the healing patterns of wounds subject to given set of therapies.

7. References

1. C. Bansal, R. Scott, D. Stewart, C.J. Cockerell, Decubitus Ulcers: A Review of the Literature, International Journal of Dermatology, 44:805-10, (2005).

2. Pressure Ulcers in America: Prevalence, Incidence and Implications for the Future. An Executive Summary of the National Pressure Ulcer Advisory Panel Monograph, Advanced Skin Wound Care, 14(4), 208-15, (2001).

3. J. Stausberg, K. Kroger, I. Maier, H. Schneider, W. Niebel, Interdisciplinary Decubitus Project. Pressure Ulcers in Secondary Care: Incidence,

Prevalence and Relevance, Advanced Skin Wound Care, 18, 140-5, (2005).

4. D. Doherty, F. Ross, L. Yeo and J. Uttley, Leg Ulcer Management in an Integrated Service, The South Thames Evidence Based Practice (STEP) Project, Report (6), Kingston University, (2000).

5. A. Fletcher, Common Problems of Wound Management in the Elderly. In Harding KG, Leaper DL, Turner TD. (eds). Proceedings of the First European Conference on the Advances in wound management. London: Macmillan, 25-29, (1992).

6. Kings Fund Grant to Help Treat Leg Ulcers, Br. Med. J., 297, 1412, (1988).

7. S. R. Carroll. Hydrocolloid Wound Dressings in the Community. Dermatol Pract, 8: 24-26, (1990).

8. N. Bosanquet, Costs of Venous Ulcers: From Maintenance Therapy to Investment Programmes, Phlebology 1992; 7(suppl): 44-46.

9. T.A. Krouskop, R. Baker and M.S. Wilson, A Noncontact Wound Measurement System, Journal of Rehabilitation Research and Development, 39(3), 337-346, (2002).

10. P. Plassmann, J.M. Melhuish and K.G. Harding, Methods of Measuring Wound Size: A Comparative Study. WOUNDS: A compendium of clinical research and practice, 6(2), 54-61, (1994).

11. R. J. Goldman, R. Salcido, More than one way to Measure a Wound: An Overview of Tools and Techniques. Advanced Skin Wound Care, 15, 236-43, (2002).

12. P. E. Houghton, C. B. Kincaid, K. E. Campbell, M. G. Woodbury, D. H. Keast, Photographic Assessment of the Appearance of Chronic Pressure and Leg Ulcers, Ostomy Wound Manage, 46(4), 28-30, (2000).

13. C. Lucas, J. Classen, D. Harrison, H. De, Pressure Ulcer Surface Area Measurement using Instant Full-Scale Photography and Transparency Tracings. Advanced Skin Wound Care, 15, 17-23, (2002).

14. M. Dyson, J. Suckling. Stimulation of Tissue Repair by Ultrasound: A survey of the mechanisms involved, Physiotherapy, 64, 105–108, (1978).

15. J. Maklebust, Pressure Ulcer Assessment, Clinics in Geriatric Medicine, 13(3), 455-81, (1997).

16. P. Plassmann, T. D. Jones, MAVIS: A Non-Invasive Instrument to Measure Area and Volume of Wounds, Measurement of Area and Volume Instrument System. Medical Engineering Physics, 20(5), 332-8, (1998).

17. M. J. Thali, M. Braun, R. Dirnhofer, Optical 3D Surface Digitizing in Forensic Medicine: 3D Documentation of Skin and Bone Injuries, Forensic Science International, 137(2-3), 203-8, (2003).

18. J. Hoschek, D. Lasser, Computer Aided Geometric Design A K Peters, (1993).

19. M. E. Mortenson, Geometric Modelling, Wiley-Interscience, New York (1985).

20. G. Farin, Curves and Surfaces for Computer Aided Geometric Design, A Practical Guide Morgan-Kaufmann, (2001).

21. C. Bajaj, J. Blinn, J. Bloomenthal, M. Cani-Gascuel, A. Rock-wood, B. Wyvill, G. Wyvill, Introduction to Implicit Surfaces Morgan-Kaufmann, (1997).

22. R. Szeliski, D. Terzopoulos, From Splines to Fractals. In Proceedings of the 16th annual conference on Computer Graphics and Interactive Techniques ACM New York, 51-60, (1989).

23. A. Rappoport, S. Spitz, Interactive Boolean Operations for Conceptual Design of 3-d Solids. In Proceedings of the 24th Annual Conference on Computer Graphics and Interactive Techniques ACM New York, 269-278, (1997).

24. T. DeRose, M. Kass, T. Truong, Subdivision Surfaces in Character Animation. In Proceedings of SIGGRAPH 98 Addison-Wesley, 85-94, (1998).

25. I. D. Faux and M. J. Pratt, Computational Geometry For Design And Manufacture, Halsted Press (Wiley), 1979.

26. G. Farin, From conics to NURBS, A Tutorial and Survey, IEEE Computer Graphics and Applications, Vol. 12, No. 5, 1992, pp. 78-86.

27. L. Piegl, Recursive Algorithms for the Representation of Parametric Curves and Surfaces, Computer Aided Design, Vol. 17, No. 5, 1985, pp. 225-229.

28. L. Piegl, The NURBS Book, Springer-Verlag, New York, 1997.

29. H. Pottmann, S. Leopoldseder, M. Hofer, T. Steiner and W. Wang, Industrial Geometry: Recent Advances and Applications in CAD, Computer Aided Design, 37(7), 751-766, (2005).

30. E. Catmull and J. Clark, Recursively Generated B-Spline Surfaces on Arbitrary Topological Meshes. Computer Aided Design, 10(6), 350-355, (1978).

31. C. T. Loop. Smooth Subdivision Surfaces based on Triangles, Master's Thesis, Department of Mathematics, University of Utah, (1987).

32. N. Dyn, D. Levine and J. A. Gregory, A Butterfly Subdivision Scheme for Surface Interpolation with Tension Control, ACM Transactions on Graphics, 9(2), 160-169, (1990).

33. A. Hubeli, and M. Gross, A survey of Surface Representations for Geometric Modeling, Computer science department, ETH Zurich, Swizerland, CS Technical report No. 335, 2000.

34. E. Catmull, Subdivision Algorithm for the Display of Curved Surfaces, PhD thesis, University Of Utah, 1974.

35. M.I.G. Bloor and M.J. Wilson, Generating Blend Surfaces using Partial Differential Equations, Computer Aided Design, 21(3), 165-171, (1989).

36. H. Du and H. Qin, A Shape Design System using Volumetric Implicit PDEs, Computer Aided Design, 36(11), 1101-1116, (2004).

37. H. Ugail, M.I.G. Bloor, and M.J. Wilson, Techniques for Interactive Design Using the PDE Method, ACM Transactions on Graphics, 18(2), 195-212, (1999).

38. L. You, P. Comninos, J.J. Zhang, PDE Blending Surfaces with C2 Continuity, Computers and Graphics, 28(6), 895-906, (2004).

39. J. Monterde and H. Ugail, A General 4th-Order PDE Method to Generate Bézier Surfaces from the Boundary, Computer Aided Geometric Design, 23(2), 208-225, (2006).

40. M.I.G., Bloor, and M.J. Wilson, Using Partial Differential Equations to Generate Freeform Surfaces, Computer-Aided Design, 22, 202-212, (1990).

41. H. Ugail, On the Spine of a PDE Surface, Mathematics of Surfaces X, M.J. Wilson and R.R. Martin (eds.), Springer, pp. 366--376, (2003).

42. R. Schneider and L Kobbelt, Geometric Fairing of Irregular Meshes for Free-Form Surface Design, Computer Aided Geometric Design, 18 (4), 359–379, (2001).

43. B. Kim and J. Rossignac, Localized Bi-Laplacian Solver on a Triangle Mesh and its Applications, Georgia Institute of Technology, GVU Technical Report Number: GIT-GVU-04-12, (2004).

44. R. Schneider, L. Kobbelt and H -P. Seidel, Improved Bi-Laplacian Mesh Fairing. In: Lyche, T., Schumaker, L.L. (Eds.), Mathematical Methods for Curves and Surfaces, Oslo, 2000, In Innovations in Applied Mathematics Series, Vanderbilt Univ. Press, pp. 44-454, (2001).

45. L. Rudin, S. Osher and E. Fatemi, Nonlinear Total Variation Based Noise Removal Algorithms, Physica D, 60(1-4), 25--268, (1992).

46. N. Paragios and R. Deriche, A PDE-Based Level Set Approach for Detection and Tracking of Moving Objects, INRIA Technical Report, INRIA, France, (1997).

47. L. A. Vese, T. F. Chan, A Multiphase Level Set Framework for Image Segmentation using The Mumford and Shah Model, International Journal of Computer Vision, 50(3), 271-293, (2002).

48. R. Schneider and L. Kobbelt, Generating fair meshes with g1 boundary conditions, In Proceedings of the Geometric Modelling and Processing 2000, IEEE, Washington, 251-261, (2000).

49. M. Desbrun, M. Meyer, P. Schroder, and A. H. Barr, Implicit Fairing of Irregular Meshes using Diffusion and Curvature Flow, In Proceedings of SIGGRAPH '99, ACM, 317-324, (1999).

50. M. J. D. Powell, The theory of radial basis function approximation in 1990, In Proceedings of 4th Summer School, Advances in numerical analysis. Vol. 2: Wavelets, subdivision algorithms, and radial basis functions, Oxford University Press, Oxford, 105--210, (1992).

51. H. Ugail, M. J. Wilson, Efficient Shape Parameterisation for Automatic Design Optimisation using a Partial Differential Equation Formulation. Computers and Structures, 81(29),2601-2609, (2003).

52. O. D. Kellogg, Foundations of Potential Theory. Dover Publications, (1969).

53. J. D. Jackson, Classical Electrodynamics, Wiley, (1999).

54. D. J. Acheson, Elementary Fluid Dynamics, Oxford University Press, (1990).

55. M. I. G. Bloor, and M. J. Wilson, Spectral Approximations to PDE Surfaces, Computer-Aided Design, 28, 145–152, (1996).

56. W.H. Press, S.A. Teukolsky, W.T. Vetterling and B.P. Flannery, Numerical Recipes in C, Cambridge University Press, (1992).